

Optimization of triangular-profiled Si-grating fabrication technology for EUV and SXR applications

© D.V. Mokhov,¹ T.N. Berezovskaya,¹ K.Yu. Shubina,¹ E.V. Pirogov,¹ A.V. Nashchekin,² V.A. Sharov,^{1,2} L.I. Goray^{1,3}

¹ Alferov University,
194021 St. Petersburg, Russia

² Ioffe Institute,
194021 St. Petersburg, Russia

³ Institute for Analytical Instrumentation,
190103 St. Petersburg, Russia
E-mail: dm_mokhov@rambler.ru

Received April 1, 2022

Revised April 1, 2022

Accepted April 1, 2022

Anisotropic wet etching of vicinal monocrystalline Si (111)4° wafers was used to obtain blazed gratings that are highly efficient in the soft X-ray (SXR) and extreme ultraviolet (EUV) applications. An improved experimental technology for the fabrication of triangular-grooved Si gratings, both medium-frequency (250 and 500 mm⁻¹) and high-frequency (2500 mm⁻¹) ones, is presented. The stages of forming a Cr-mask for grooves etching, removing Si nubs in order to smooth the profile, and polishing the surface to reduce nanoroughness have been optimized. This paper describes the way of simultaneously (in one process) obtaining a smoothed triangular profile of the Si grating and a polished surface of facets by wet etching.

Keywords: diffraction grating, Si wet etching, triangular groove profile, AFM, SEM.

DOI: 10.21883/TP.2022.08.54564.74-22

Introduction

Wet anisotropic etching of grooves in single-crystal Si(111) with misorientation, which was for the first time proposed by the authors of [1], is being exploited and optimized for fabricating blazed reflective gratings by many researchers [2–5]. Anisotropic etching in KOH results in formation of silicon nubs that reduce the reflective facet length, obscure the adjacent facet, and interfere the atomic flux during depositing the reflective coating. To remove the Si nubs, smoothing etching is performed in the form of a multi-stage procedure consisting of several (9–26) cycles of treatment in etchants (piranha/HF [6] or RCA-1/HF [4]). We process the Si grating to remove the Si nubs with a smoothing etchant in one stage with a short etching duration, and then with a polishing etchant in order to reduce the surface roughness of reflective facets [7].

The task of this study was to find an etchant able to simultaneously (in one process) smooth the profile and polish the surface. Variations in the Si grating profile and reflective facet roughness after anisotropic KOH-etching and subsequent treatment with smoothing–polishing etchants were studied using scanning electron microscopy (SEM) and atomic force microscopy (AFM).

1. Formation of the protective mask

The Cr-mask can be formed on the Si substrate surface in different ways. In fabricating a triangular-profiled grating, the authors of [8] obtained the chrome mask by reactive

ion etching through a resist mask. In our experiments on fabricating the medium-frequency triangular-profiled Si grating, we prepared the Cr-mask by wet etching of chrome in a cerium etchant through a photoresist mask [9]. Practical limits of applicability of the wet chemical etching (WCE) are defined by its resolution (1.5–2.0 μm) and size variation during etching (0.2–0.5 μm). Although the time necessary for obtaining the Cr-mask by wet etching of a chrome layer 20–30 nm thick is not long (20–30 s), the lateral undercut under the Cr strip appears to be quite large (up to 0.2 μm) as compared with the preset width (1 μm) of Cr strips on the photoresist mask for a medium-frequency grating 2 μm in period. In fabricating high-frequency gratings (100–500 nm in period), the WCE method is not applicable to the Cr-mask formation since in this case the width of protective Cr strips is very low (40–200 nm). Therefore, instead of obtaining the Cr-mask by WCE, we used the „lift-off“ technique suitable for gratings of various periods ranging from ~ 0.1 to ~ 10 μm.

Regardless of the method for forming the protective mask, it is very important to choose the optimal width of Cr strips on the Cr-mask for Si gratings with different periods: not too narrow so that protection during KOH-etching is provided, and not too wide so that Si nubs are not exceedingly large, since otherwise a longer smoothing-etching time will be required to remove them. During the KOH-etching, lateral undercut of silicon under the Cr-mask takes place; this results in a decrease in the width of the area of the Cr strip adhesion to the silicon surface (by 0.04–0.4 μm, depending on the etching duration); this is why the width

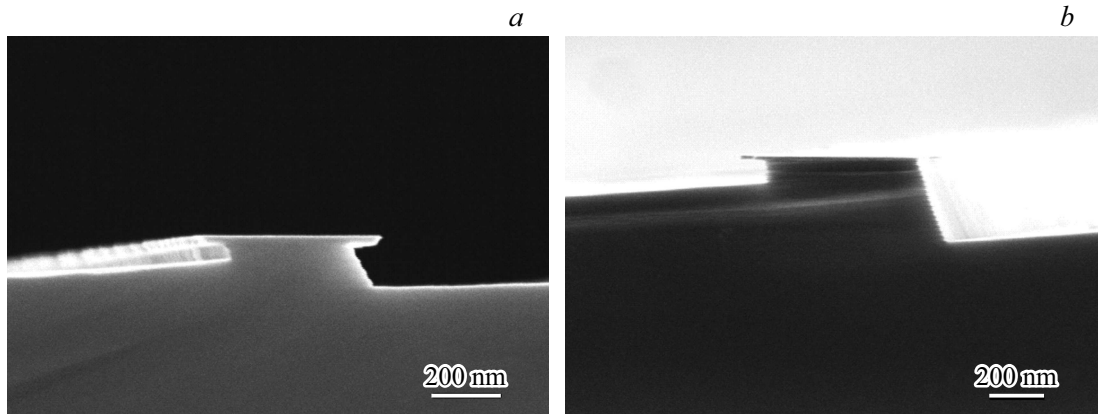


Figure 1. SEM image of the Cr-mask after anisotropic KOH-etching of the Si grating: *a* — period of $2\mu\text{m}$, *b* — period of $4\mu\text{m}$.

of protective Cr strips should be sufficient to prevent the Cr strip detachment. The greater is the etching depth (and, hence, the etching time), the greater is the Cr-mask lateral undercut. Fig. 1 presents an image of the Cr-mask fabricated by the lift-off method; the image was obtained by SEM after KOH-etching.

2. Smoothing-polishing of the surface

Anisotropic KOH-etching of grooves, as well as smoothing etching for removing Si nubs, should not reduce the surface quality. This requires careful optimization of the grating etching procedures. To reduce roughness of the Si-grating reflective surfaces, different techniques are used, for instance, adding surfactants to the etchant [10]. Anisotropic etching in the NH_4F solution can provide an atomically smooth surface [11] with the root-mean-square (RMS) roughness of 1.1 \AA [5].

Notice that the polished surfaces RMS roughness of the used $\text{Si}(111)4^\circ$ substrates is $\sim 0.15\text{ nm}$ ($1 \times 1\mu\text{m}^2$, 512 points per scan); values of the similar parameter reported by different authors vary from ~ 0.1 [5] to $\sim 0.3\text{ nm}$ [12].

The technique of anisotropic KOH etching which we have optimized for samples of a small size ($\sim 10 \times 15\text{ mm}^2$) [9] was applied to large-size samples (the whole Si wafer with $\text{Ø}76.2\text{ mm}$ or its half). After anisotropic KOH-etching of grooves, large samples exhibited an increase in the surface roughness, mainly medium-frequency one, which manifested itself as waviness and retained even after removing the Si nubs (Fig. 2). The surface roughness standard deviation was $1.2\text{--}1.5\text{ nm}$ (field of $1 \times 1\mu\text{m}^2$, 512 points in a one-dimensional scan) and $3.0\text{--}5.5\text{ nm}$ ($20 \times 20\mu\text{m}^2$), which is unacceptable for the X-ray diffraction grating.

The technique we used earlier implied that, after KOH-etching of grooves and removal of the Cr-mask, the Si grating is placed first into a smoothing etchant to eliminate the Si nubs and then into a polishing etchant to reduce the surface roughness. Based on the results of surface polishing experiments in our previous work,

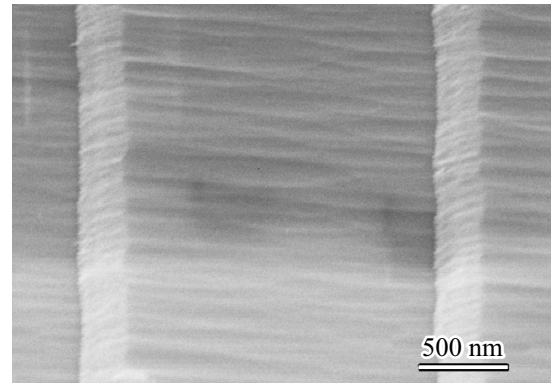


Figure 2. SEM image of the Si grating after removing Si nubs.

polishing etchant TMAH was chosen [7]. After polishing with TMAH, standard deviation of the Si grating surface roughness was $\sim 0.25\text{--}0.34\text{ nm}$ ($1 \times 1\mu\text{m}^2$); this value is satisfactory for applying an appropriate reflective coating on the EUV–SXR Si grating. In the EUV range, the acceptable grating surface roughness was assumed to be $\sim 0.4\text{--}1\text{ nm}$ [6]; that in the soft X-ray (SXR) range was $\sim 0.3\text{--}0.4\text{ nm}$ [4,13].

As an optimal technological solution, it is preferable to choose such an etchant that enables simultaneously (in one process) performing both the Si nubs removal and surface polishing (elimination of waviness, i.e. the medium-frequency roughness). Section 2 presents the results of continuing our experiments on the Si-grating profile smoothing and surface polishing with etchants able to simultaneously remove from the surface both the Si nubs and smaller irregularities (waviness) without distorting the triangular profile and violating the reflective facet flatness (without surface camber).

A Si-grating sample (Fig. 3) with Si nubs whose average height, after the anisotropic KOH-etching and Cr-mask removal, equaled $\sim 83\text{ nm}$, was divided into 4 fragments intended for studying the processes of the profile smoothing

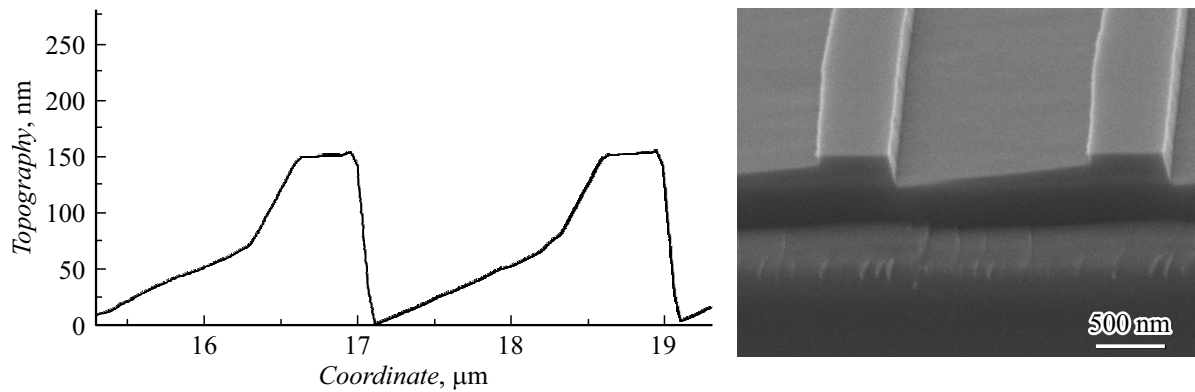


Figure 3. AFM profile and SEM image of the Si grating after anisotropic KOH-etching and Cr-mask removal; the Si nub height is 83 nm.

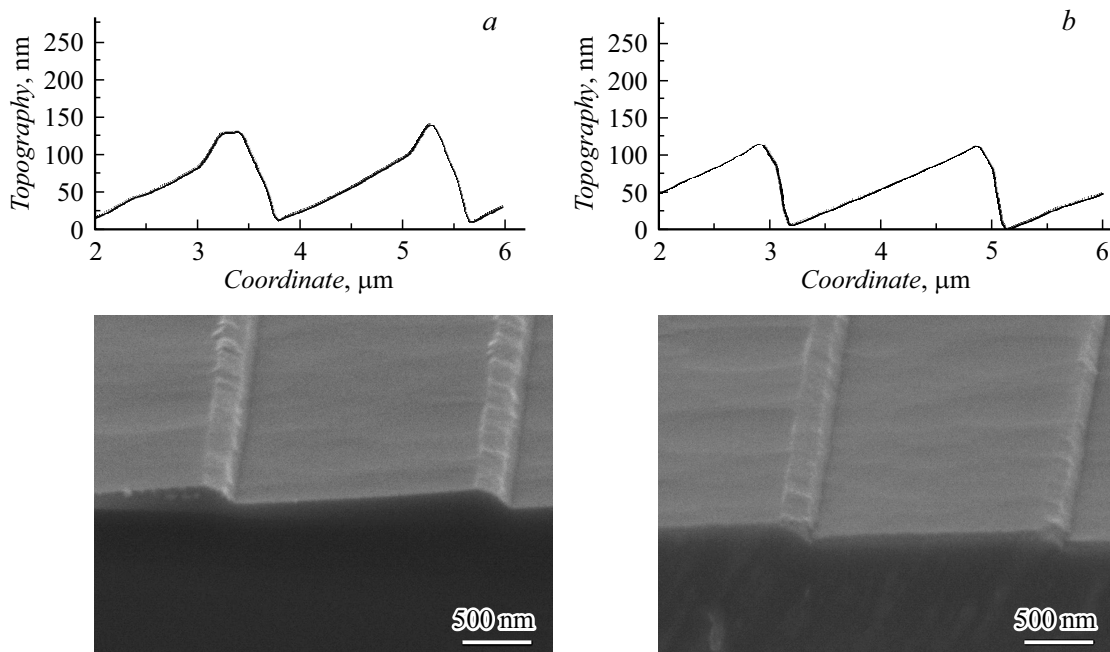


Figure 4. AFM profiles and SEM images after processing with etchant #1: *a* — without surfactants; *b* — with surfactants.

and surface polishing. The fragments were treated in different ways:

1) in an alkaline inorganic etchant (hereinafter referred to as etchant #1) without adding a surfactant (fragment #1) and with adding a surfactant (fragment #3) (Fig. 4);

2) in an alkaline organic etchant (hereinafter referred to as etchant #2) in one step (fragment #2) and in two steps (fragment #4) (Fig. 5);

3) with two etchants in sequence: fragment #1 processed with etchant #1 without adding a surfactant was then processed with etchant #2 (Fig. 6).

The AFM profiles and SEM images of fragments ## 1–4 after processing are presented in Figs. 4–6; measurements of the reflective facet parameters are listed in the Table.

Fig. 4 illustrates two cases of treatment with etchant #1, each of the same duration: in case the surfactant is not added, the Si nubs are not fully removed, the maximum

height of remaining Si nubs being ~ 34 nm (Fig. 4, *a*), while in case the surfactant is added, the Si nubs are removed and the profile is smoothed (Fig. 4, *b*). The presence of surfactants in the solution promotes an increase in the rate of Si nubs etching, as well as reduction of the surface roughness.

As shown in Fig. 5, treatment with etchant #2 performed with the same duration in one stage (Fig. 5, *a*) and in two stages (Fig. 5, *b*) provides complete removal of Si nubs with a significant reduction of surface roughness.

To ensure complete removal of the remaining Si nubs, the sample pretreated with etchant #1 without adding surfactants (Fig. 4, *a*) was then processed with etchant #2, after which the Si nubs appeared to be fully removed and the profile got smoothed (Fig. 6).

Based on the results of studying the processes of smoothing–polishing the medium-frequency grating,

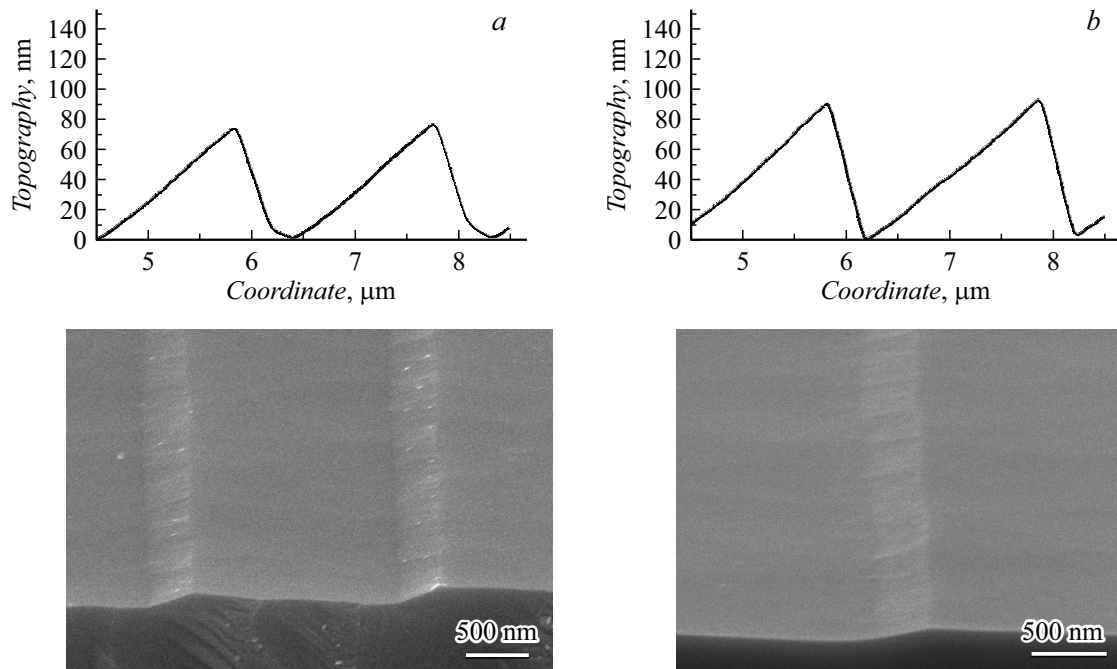


Figure 5. AFM profiles and SEM images after processing with etchant #2: *a* — in one step, *b* — in two steps.

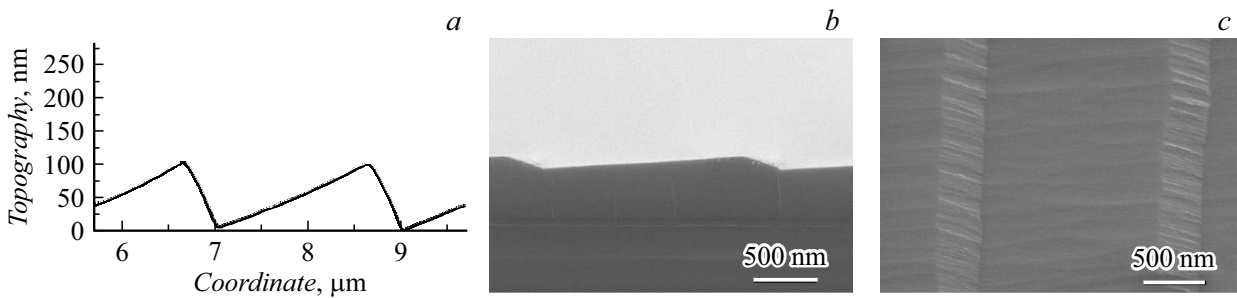


Figure 6. AFM profiles and SEM images of the fragment after processing with etchant #1 without adding a surfactant and subsequent processing in etchant #2.

Parameters of reflective facets of the Si-grating fragments, period of 2 μm

Grating fragment #	Chemical treatment	Number of steps	Reflective facet parameters		
			Length, nm	Camber, $C, ^\circ$	RMS ($1 \times 1 \mu\text{m}^2$)
Source	KOH-etching	1	1064	0.04	1.12
1	Etchant #1 free of surfactant	1	1750	0.67	0.58
3	Etchant #1 with surfactant	1	1586	0.27	0.46
2	Etchant #2	1	1251	0.24	0.21
4	Etchant #2	2	1520	0.38	0.24
1	Etchant #1 free of surfactant and etchant #2	2	1542	0.45	0.36

etchant #1 with surfactant was chosen for using in fabricating the high-frequency Si grating 400 nm in period to remove Si nubs 28–37 nm high. In selecting the etchant, not only the RMS roughness magnitude was taken into

account, but also other reflective facet parameters (length and flatness) affecting the grating diffraction efficiency (see the Table). AFM profiles of the high-frequency grating at different stages of fabrication are demonstrated in Fig. 7.

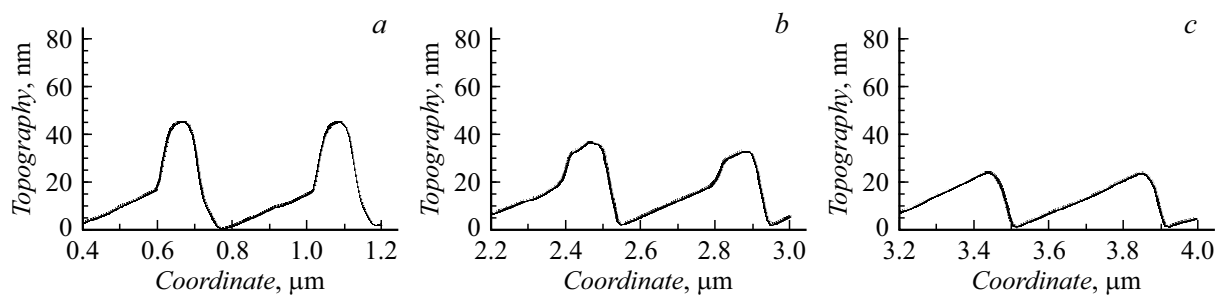


Figure 7. AFM profiles of a Si-grating after etching: *a* — in KOH, Cr-mask removed, Si nub height 28 nm; *b* — in etchant #1 with surfactant, Si nub height 11 nm; *c* — additional treatment with etchant #1 with surfactant.

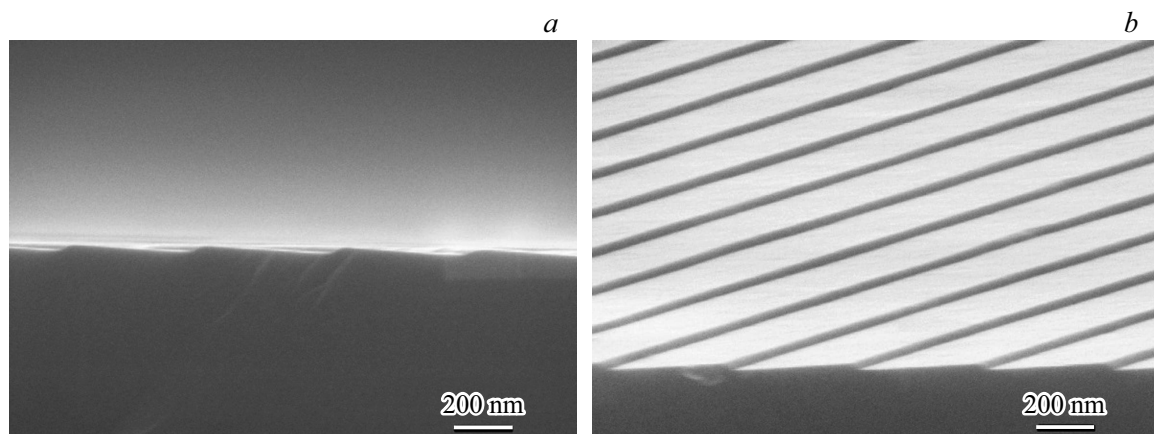


Figure 8. SEM images of the finished Si grating, period 400 nm: *a* — cross-section; *b* — isometry, angle 10°.

After the smoothing-polishing etching with etchant #1 with surfactant, the high-frequency Si grating exhibits the following parameters: working facet length of 314 nm, groove depth of 21 nm, measured surface RMS roughness of 0.78 nm ($4 \times 4 \mu\text{m}^2$). Fig. 8 presents SEM images of the finished Si grating with a smoothed profile.

3. Conditions for achieving high diffraction efficiency of the Si grating

High diffraction efficiency of gratings operating in high spectrum orders in the SXR and EUV ranges gets achieved due to ensuring proper quality of formation of the grating reflective facets in the process of fabrication [9]. The procedure for manufacturing the blazed grating should ensure attaining optimal reflective facet parameters, namely, the absence of Si nubs, large length, flatness (lack of camber) and low roughness, which is governed by the conditions of the anisotropic etching of grooves, as well as of the smoothing and polishing etching.

We have studied the influence of random roughness on the grating reflectivity by simulation with the PCGrate program code; based on the known Debye-Waller or Nevot-Croce approximation, the following estimate of acceptable roughness not affecting the reflection coefficients of the SXR-EUV radiation was obtained: the RMS roughness

should not exceed 0.5 nm. We use this criterion in practical work.

To select the smoothing-polishing etchant and find the optimal processing mode, parameters of the reflective facet were determined from AFM profiles of the studied Si-grating fragments (see the Table). The camber indicator (C) was assumed to be the difference between the slope angles of the reflective facet top and bottom measured for the top taking into account „30% points at the facet top“ and for the bottom taking into account „30% points at the facet bottom discarding 10% of points from the lowest point“; the C measurement unit was angular degree. The calculated value of C is compared with the measurement error of the reflective facet slope angle based on processing the AFM profiles measured at a length of 10 periods in two areas separated from each other by at least 1000 periods. The Table shows that the reflective facet length increased by 18–49% due to the Si nubs removal, while the RMS roughness decreased to acceptable values due to surface polishing.

Thus, the variable conditions of the smoothing and polishing etching are the etchant chemical composition and concentration, processing temperature, sample orientation during etching (vertical or horizontal), stirring conditions, number and duration of the processing stages, and the sequence of treating with etchants. The future experiments

will be aimed at selecting optimal conditions for the smoothing and polishing (or smoothing-polishing) etching, which could reproducibly provide the best reflective facet parameters: length, camber and roughness.

Conclusion

Thus, the assigned task, that is, performing the smoothing and polishing etching simultaneously in one process has been successively accomplished for different frequencies of the fabricated SXR–EUV gratings (periods of 0.4, 2 and 4 μm). Thereat, there were obtained a smoothed triangular profile free of Si nubs and an even, clean and smooth surface with acceptable roughness: the measured RMS roughness varied from 0.21 to 0.58 nm ($1 \times 1 \mu\text{m}^2$). Our further efforts will be aimed at optimizing the smoothing-polishing etching conditions so as to obtain the best working facet parameters defining the diffraction efficiency, and also at studying the dependence of the Si-grating diffraction characteristics on the working facet parameters. In addition, there should be performed optimization of the design efficiency of diffraction gratings with the measured groove profiles operating in various spectral ranges, orders and diffraction schemes (classical or conical) [14–16]. The efficiency measurements are expected to confirm the validity and reliability of the selected optimization procedures.

Financial support

In terms of experimental studies, the work was supported by the Russian Foundation for Basic Research (RFBR) (project 20-02-00326). The theoretical part of work of L.I. Goray, A.S. Dashkov, D.V. Mokhov, E.V. Pirogov and K.Yu. Shubina was supported by the Russian Science Foundation (19-12-00270-P).

Conflict of interests

The authors declare that they have no conflict of interests.

References

- [1] P. Philippe, S. Valette, M. Mendez, D. Maystre. *Appl. Opt.*, **24** (7), 1006 (1985). DOI: 10.1364/AO.24.001006
- [2] A.E. Franke, M.L. Schattenburg, E.M. Gullikson, J. Cottam, S.M. Kahn, A. Rasmussen. *J. Vac. Sci. Technol. B*, **15**, 2940 (1997). DOI: 10.1116/1.589759
- [3] D.M. Miles, J.A. McCoy, R.L. McEntaffer, C.M. Eichfeld, G. Lavallee, M. Labella, W. Drawl, B. Liu, C.T. DeRoo, T. Steiner. *Astrophys. J.*, **869** (2), 12 (2018). DOI: 10.3847/1538-4357/aacc73
- [4] L. Golub, P. Cheimets, E.E. DeLuca, C.A. Madsen, K.K. Reeves, J. Samra, S. Savage, A. Winebarger, A.R. Brucoleri. *J. Space Weather Space Clim.*, **10**, 37 (2020). DOI: 10.1051/swsc/2020040
- [5] D.L. Voronov, R. Cambie, E.M. Gullikson, V.V. Yashchuk, H.A. Padmore, Y.P. Pershin, A.G. Ponomarenko, V.V. Kondratenko. *Proc. SPIE*, **7077**, 12 (2008). DOI: 10.1117/12.795377
- [6] D.L. Voronov, E.H. Anderson, R. Cambie, F. Salmassi, E.M. Gullikson, V.V. Yashchuk, H.A. Padmore, M. Ahn, C.-H. Chang, R.K. Heilmann, M.L. Schattenburg. *Proc. SPIE*, **7448**, 74480J (2009). DOI: 10.1117/12.82692
- [7] D.V. Mokhov, T.N. Berezovskaya, E.V. Pirogov, A.V. Nashchokin, V.A. Sharov, L.I. Goray. *Tez. dokl. conf. KELT-2021* (Chernogolovka, Russia, 2021), p. 291. (in Russian).
- [8] U.D. Zeitner, T. Fugel-Paul, T. Harzendorf, M. Heusinger, E.-B. Kley. *Spectrometer Gratings Based on Direct-Write e-Beam Lithography* [Electronic resource] Available at: <http://www.brera.inaf.it/DispersingElements2017/slides/Zeitner.pdf>, free (date of application: 27.04.2022).
- [9] L.I. Goray, T.N. Berezovskaya, D.V. Mokhov, V.A. Sharov, K.Yu. Shubina, E.V. Pirogov, A.S. Dashkov. *ZhTF*, **91** (10), 1538 (2021). (in Russian) DOI: 10.21883/JTF.2021.10.51368.81-21
- [10] M. Ahn, R.K. Heilmann, M.L. Schattenburg. *J. Vac. Sci. Technol. B*, **26** (6), 2179 (2008). DOI: 10.1364/OE.16.008658
- [11] S.-E. Bae, M.-K. Oh, N.-K. Min, S.-H. Paek, S.-I. Hong, Ch.-W.J. Lee. *Bull. Korean Chem. Soc.*, **25** (12), 1822 (2004). DOI: 10.33961/jecst.2020.00920
- [12] B. Sheng, X. Xu, Y. Liu, Y. Hong, H. Zhou, T. Huo, S. Fu. *Opt. Lett.*, **34** (8), 1147 (2009). DOI: 10.1364/OL.34.001147
- [13] F. Salmassi, P.P. Naulleau, E.M. Gullikson, D.L. Olynick, J.A. Liddle. *J. Vac. Sci. Technol. A*, **24** (4), 1136 (2006). DOI: 10.1116/1.2212435
- [14] D.L. Voronov, M. Ahn, E.H. Anderson, R. Cambie, Ch.-H. Chang, L.I. Goray, E.M. Gullikson, R.K. Heilmann, F. Salmassi, M.L. Schattenburg, T. Warwick, V.V. Yashchuka, H.A. Padmore. *Proc. SPIE*, **7802**, 780207 (2010). DOI: 10.1117/12.861287
- [15] L. Goray, M. Lubov. *J. Appl. Cryst.*, **46**, 926 (2013). DOI: 10.1107/S0021889813012387
- [16] L. Goray, W. Jark, D. Eichert. *J. Synchrotron Rad.*, **25**, 1683 (2018). DOI: 10.1107/S1600577518012419